





# The hedgehog pathway suppresses neuropathogenesis in CD4 T cell-driven inflammation

Nail Benallegue,<sup>1,2,†</sup> Hania Kebir,<sup>1,†</sup> Richa Kapoor,<sup>1,†</sup> Alexis Crockett,<sup>1</sup>  Gen Li,<sup>1,3</sup> Lara Cheslow,<sup>1</sup> Mohamed S. Abdel-Hakeem,<sup>4,5,6</sup> James Gesualdi,<sup>1</sup> Miles C. Miller,<sup>1</sup> E. John Wherry,<sup>4,5</sup> Molly E. Church,<sup>1</sup> M. Andres Blanco<sup>7</sup> and  Jorge I. Alvarez<sup>1</sup>

<sup>†</sup>These authors contributed equally to this work.

The concerted actions of the CNS and the immune system are essential to coordinating the outcome of neuroinflammatory responses. Yet, the precise mechanisms involved in this crosstalk and their contribution to the pathophysiology of neuroinflammatory diseases largely elude us.

Here, we show that the CNS-endogenous hedgehog pathway, a signal triggered as part of the host response during the inflammatory phase of multiple sclerosis and experimental autoimmune encephalomyelitis, attenuates the pathogenicity of human and mouse effector CD4 T cells by regulating their production of inflammatory cytokines.

Using a murine genetic model, in which the hedgehog signalling is compromised in CD4 T cells, we show that the hedgehog pathway acts on CD4 T cells to suppress the pathogenic hallmarks of autoimmune neuroinflammation, including demyelination and axonal damage, and thus mitigates the development of experimental autoimmune encephalomyelitis. Impairment of hedgehog signalling in CD4 T cells exacerbates brain-brainstem-cerebellum inflammation and leads to the development of atypical disease. Moreover, we present evidence that hedgehog signalling regulates the pathogenic profile of CD4 T cells by limiting their production of the inflammatory cytokines granulocyte-macrophage colony-stimulating factor and interferon- $\gamma$  and by antagonizing their inflammatory program at the transcriptome level. Likewise, hedgehog signalling attenuates the inflammatory phenotype of human CD4 memory T cells.

From a therapeutic point of view, our study underlines the potential of harnessing the hedgehog pathway to counteract ongoing excessive CNS inflammation, as systemic administration of a hedgehog agonist after disease onset effectively halts disease progression and significantly reduces neuroinflammation and the underlying neuropathology. We thus unveil a previously unrecognized role for the hedgehog pathway in regulating pathogenic inflammation within the CNS and propose to exploit its ability to modulate this neuroimmune network as a strategy to limit the progression of ongoing neuroinflammation.

- 1 Department of Pathobiology, School of Veterinary Medicine, University of Pennsylvania, Philadelphia, PA 19104, USA
- 2 Inserm, Université de Nantes, CHU Nantes, Centre de Recherche en Transplantation et Immunologie, UMR 1064, ITUN, F-44000 Nantes, France
- 3 Northwest Institute of Plateau Biology, Chinese Academy of Sciences, Xining 810008, China
- 4 Institute for Immunology, Perelman School of Medicine, University of Pennsylvania, Philadelphia, PA 19104, USA
- 5 Department of Systems Pharmacology and Translational Therapeutics, School of Medicine, University of Pennsylvania, Philadelphia, PA 19104, USA
- 6 Department of Microbiology and Immunology, Faculty of Pharmacy, Cairo University, Kasr El-Aini, Cairo 11562, Egypt

Received June 21, 2020. Revised December 08, 2020. Accepted December 17, 2020. Advance access publication March 16, 2021

© The Author(s) (2021). Published by Oxford University Press on behalf of the Guarantors of Brain. All rights reserved.

For permissions, please email: journals.permissions@oup.com

7 Department of Biomedical Sciences, School of Veterinary Medicine, University of Pennsylvania, Philadelphia, PA 19104, USA

Correspondence to: Jorge I. Alvarez, PhD  
Department of Pathobiology, School of Veterinary Medicine, University of Pennsylvania  
380 South University Avenue, 412 Hill, Philadelphia, PA 19104, USA  
E-mail: [alvaj@vet.upenn.edu](mailto:alvaj@vet.upenn.edu)

**Keywords:** sonic hedgehog; neuroinflammation; autoimmunity; experimental autoimmune encephalomyelitis; T cells

**Abbreviations:** EAE = experimental autoimmune encephalomyelitis; GM-CSF = granulocyte-macrophage colony-stimulating factor; Hh = hedgehog; IFN = interferon; IL = interleukin

## Introduction

Multiple sclerosis is a chronic neuroinflammatory disease with a mixed clinical presentation, possibly due to the heterogeneous distribution of demyelinating plaques within the CNS.<sup>1</sup> Multiple sclerosis lesion sites are characterized by astrogliosis, demyelination, blood–brain barrier damage and axonal degeneration thought to result from an aberrant and persistent immune cell response within the CNS.<sup>2–4</sup> The development of acute multiple sclerosis lesions, especially in its most common relapsing–remitting form, is marked by perivascular accumulation of pathogenic T cells, including pro-inflammatory effector memory T helper (Th) 1 and Th17 lymphocytes that migrate from the periphery to the CNS across the blood–brain barrier.<sup>5–7</sup> However, as the disease evolves, the inflammatory process appears to become more insulated from the periphery and mostly confined to the CNS. Increasing evidence suggests that CNS signals, released as part of the host response, play defining roles in mitigating immune cell function within the brain compartment.<sup>8,9</sup> Yet, the exact CNS-intrinsic pathways that actively participate in the resolution of inflammation in multiple sclerosis and its animal model, experimental autoimmune encephalomyelitis (EAE), remain ill defined. In this regard, sonic hedgehog (SHH), the main ligand of the hedgehog (Hh) signalling pathway, was shown to be markedly upregulated by astrocytes within multiple sclerosis and EAE lesions, where its main ascribed role thus far has been to induce and maintain blood–brain barrier properties through its action on the microvascular endothelium.<sup>10,11</sup>

Beside its function in embryonic neural development, the Hh pathway also plays an important role in adult tissue homeostasis,<sup>12</sup> including the CNS.<sup>13</sup> The pathway becomes activated after one of the three ligands, SHH, Indian hedgehog (IHH) or Desert hedgehog (DHH), binds to the cell surface receptor patched 1 or patched 2.<sup>14</sup> This alleviates the patched repression of the signal transducer smoothed (SMO), which then activates transcription factors of the glioma-associated antigen oncogene. T cells express Hh pathway constituents, and signalling can influence distinct stages of T-cell development,<sup>15,16</sup> modulate their activation and regulate the differentiation of effector populations.<sup>17,18</sup> The Hh pathway was also shown to regulate chronic inflammation in the gut, skin, liver and lung.<sup>19–23</sup> Moreover, Hh modulation influences the immune suppressive tumour microenvironment in models of basal cell carcinoma and breast cancer.<sup>24,25</sup> Unlike IHH and DHH, SHH is expressed in the healthy adult brain<sup>26,27</sup> and is upregulated at active lesion sites in multiple sclerosis and EAE.<sup>10,28</sup> Nevertheless, little is known about the contribution of the Hh pathway, if any, in regulating immune T-cell function during neuroinflammation.

The aim of this study was to determine how Hh signalling in CD4 T cells impacts inflammation-associated neuropathology in a

model of CNS autoimmunity. We demonstrate that the Hh pathway is a key CNS-intrinsic regulator of T-cell function and represents a potential target for therapeutic intervention of uncontrolled neuroinflammation.

## Materials and methods

### Ethical statement

All human experiments were conducted under approval of the Institutional Review Board of the University of Pennsylvania. All animal experiments were conducted in accordance with guidelines established by the Institutional Animal Care and Use Committee at the University of Pennsylvania.

### Study design

This study investigates the role of the Hh pathway in CD4 Th cells infiltrating the CNS during multiple sclerosis and EAE. We performed flow cytometry and RNA sequencing of effector CD4 T cells isolated from the CNS of EAE mice and studied the effect of Shh on human effector memory CD4 T cells. A mouse model (CD4<sup>Cre</sup>Smo<sup>o/c</sup>) was generated and characterized, with a minimum of three independent *in vivo* experiments. Experiments related to the SMO agonist were repeated four times, independently. Clinical scoring was blinded. The peak/ascending phase of the disease was the time point selected for analysis in all EAE experiments. Immunofluorescent and histopathological analyses of murine CNS tissue were performed blinded in at least five mice per genotype. For cultures of primary human effector memory T cells, Hh stimulation was performed at Days 0, 2 and 4. Sample size and collection of cells at end point was determined according to our previously published experience. Experiments using healthy volunteer peripheral blood mononuclear cell samples were carried out six times, independently.

### Mice

We made use of the Cre-LoxP methodology to inactivate *Smo* specifically in CD4 T cells. We targeted CD4 T cells with the CD4 Cre mouse line [Tg(Cd4-cre)1Cwi] generated by Christopher B. Wilson and purchased from JAX. *Smo*<sup>tm2A<sup>mc</sup>/J</sup> mice were generated by Andrew P. McMahon and purchased from JAX. We crossed mice heterozygous for CD4-Cre and mice homozygous for the conditional floxed *Smo* (*Smo*<sup>o/c</sup>). After crossing, we generated mice conditionally missing functional *Smo* within the CD4 T cell compartment (hereafter CD4<sup>Cre</sup>Smo<sup>o/c</sup>) and littermate controls (*Smo*<sup>o/c</sup>) denoted as wild-type. Mice were genotyped by PCR (Supplementary Fig. 1A). All experiments were conducted in

accordance with guidelines established by the Institutional Animal Care and Use Committee at the University of Pennsylvania.

### Hh agonists

Recombinant human SHH (100 ng/ml, R&D), recombinant mouse SHH (100 ng/ml, BioLegend) and SMO agonist (3 nM, Selleck Chemicals LLC) were used to stimulate the Hh pathway *in vitro*. For *in vivo* experiments, the SMO agonist was used at a concentration of 20 µg/g of mouse weight and reconstituted in sterile water.

### EAE

Active EAE was induced as previously reported<sup>10</sup> (Supplementary material). Mice that developed classical EAE symptoms were scored as follows: 0, asymptomatic; 1 = complete limp tail; 2 = loss of the righting reflex; 3 = waddling gait with weakness of hindlimbs; 3.5 = complete paralysis of one hindlimb; 4 = complete paralysis of both hindlimbs; 5 = complete paralysis of the four limbs or death. The scoring of non-classical EAE was adapted from previously described clinical phenotypes<sup>29,30</sup>: score 1 = slightly tilted head; 2 = moderate tilted head; 2.5 = spinning when held by the tail; 3 = severe ataxia and mouse unable to walk in a straight line; 4 = mouse needs to lean on the wall of the cage to walk or spins continuously when flipped by the tail; 5 = mouse rolls spontaneously. Representative animals from each group were euthanized at the peak of the disease and immune cells were isolated from the recovered spleen and CNS (brain and spinal cord) tissue as previously described<sup>10,11</sup> (Supplementary material). SMO agonist was administered intraperitoneally on the first day of EAE onset. Controls were given saline solution intraperitoneally. Animals were monitored as described above and euthanized 5–6 days after disease onset. Tissues were harvested and processed for flow cytometry and immunohistochemistry (Supplementary material).

### Immunofluorescence

Sagittal brain sections (8 µm) mounted on positively charged slides (ThermoFisher) were fixed in ice cold acetone and 70% ethanol and then permeabilized with Tris-buffered saline (TBS)-1 × containing 0.025% Tween 20 (Amresco). Non-specific binding was blocked with 10% normal donkey serum (Sigma) for 90 min at room temperature in a humid chamber. The following primary antibodies were diluted in 3% normal donkey serum and incubated overnight at 4°C: rabbit anti-rat/mouse fibrinogen (1:300; Innovative research), mouse anti-mouse GFAP (1:2000; Sigma), rat anti-mouse CD4 (1:50, BioLegend), rat anti-mouse CD68 (1:70, BioLegend) and rat anti-mouse VCAM-1 (1:70, BioLegend). Sections were washed with TBS-1 × and subsequently incubated with secondary antibodies (Alexa Fluor<sup>®</sup> 488 goat anti-rat IgG, Alexa Fluor<sup>®</sup> 594 donkey anti-rabbit IgG; Jackson ImmunoResearch). These were all diluted 1:300 in 3% normal donkey serum (Sigma) for 2 h in a humid chamber at room temperature. Nuclei were permeabilized with TBS-1 × and 1:100 Triton<sup>™</sup> X-100 (Amresco) for 10 min, and slides were mounted with Mowiol<sup>®</sup> media containing Hoechst nuclear dye (1:1000; BD Biosciences). Immunostained sections were imaged on a Leica widefield microscope (Leica Microsystems). Images were processed using Leica Application Suite X and Adobe Photoshop. To determine the extent of T-cell extravasation, infiltrates of CD4 T cells in the meninges and parenchymal areas of the forebrain region were quantified using Leica Application Suite X. Similar areas were studied for quantification of fibrinogen, VCAM1, CD68 and GFAP using Image J. Extravascular fibrinogen, endothelial VCAM1 expression, myeloid cell CD68 and astrocytic GFAP were quantified as integrated density in the infiltrate area (mean of the number of pixels per unit area of the infiltrate). All analyses were performed blinded.

### Histological staining

Luxol fast blue-haematoxylin and eosin staining was performed as previously published.<sup>7</sup> Frozen brain sections were fixed with 10% formalin for 6–10 h at room temperature, washed twice with distilled water, dipped in 70% ethanol and then in 95% ethanol. Paraffin-embedded sections were deparaffinized and hydrated in distilled water. All slides were placed in Luxol fast blue overnight in an oven at 60°C. Slides were then decolourized in 70% alcohol and washed with distilled water, followed by staining in Harris haematoxylin for 15 min. Acid alcohol and 1% ammonia water were used for differentiation. Then, slides were dehydrated in 95% ethanol and immersed in alcoholic eosin Y for 2 min. Slides were dehydrated (in 95% ethanol for 1 min, absolute ethanol four times at 1 min each time and xylene twice for 1 min each time) and mounted in Cytoseal<sup>™</sup> (Fisher). Saturated lithium carbonate was used as an additional differentiator for the paraffin sections.

For axonal pathology, Bielschowsky silver staining was used. Paraffin-embedded and frozen sections were fixed as indicated above. Slides were stained in 20% silver nitrate solution for 15 min at 37°C, washed with distilled water and dipped in ammoniacal silver (concentrated ammonium hydroxide in silver nitrate solution) for 15 min at 37°C. Then, slides were placed in 1% ammonium hydroxide solution for 3 min. Sections were treated with a developing solution (10% formalin, concentrated nitric acid, citric acid and distilled water), dipped in 1% ammonium hydroxide solution. Slides were then placed in 5% sodium thiosulphate solution for 5 min. Slides were dehydrated (in 95% ethanol for 1 min, absolute ethanol four times for 1 min each time and xylene twice for 1 min each time) and mounted in Cytoseal<sup>™</sup>. Stainings were imaged on a Leica widefield microscope (Leica Microsystems) and processed using Adobe Photoshop.

### Neuroinflammatory assessment

The pathological EAE scoring system was carried out in the SMO agonist- and vehicle-treated mice by evaluating three to five of the most significantly affected areas in high power fields (40 ×) for brain and spinal cord sections stained with Luxol fast blue-haematoxylin and eosin. CNS inflammation in brain (forebrain/midbrain, cerebellum and brainstem) and spinal cord was evaluated semi-quantitatively based on the severity of inflammation using the following scale: 0 = no inflammation; 1 = mild cellular infiltrates only in the perivascular areas (0–10 cells/high power field) and meninges with no or minimal degeneration of the adjacent white matter; 2 = mild cellular infiltrates in the meninges and parenchyma (11–50 cells/high power field) with mild degeneration of the affected white matter; 3 = moderate cellular infiltrates in the meninges and parenchyma (51–100 cells/high power field) with moderate degeneration of the affected white matter; 4 = marked cellular infiltrates in the meninges and parenchyma (101–200 cells/high power field) with marked degeneration of the affected white matter; 5 = severe cellular infiltrates in the meninges and parenchyma (>201 cells/high power field) with extensive degeneration of the affected white matter (for brain and/or inflammation in midbrain); 6 = 4 or 5 plus inflammation in the cerebrum. Three to five fields in the brain and spinal cord were averaged and each value was denoted for the analysis. A Board-certified veterinary pathologist (M.E.C.) evaluated the CNS slides blindly.

### Neuropathological scoring

Semi-quantitative histopathological evaluation based on the severity of myelin loss was performed in the white matter of the spinal cord, cerebellum and brainstem. The severity of demyelination was denoted using the following scale: 0 = no demyelination; 1 = small focal area of demyelination; 2 = small multifocal areas of

demyelination; 3 = large multifocal to coalescing areas of demyelination and 4 = extensive demyelination involving > 20% of the white matter using low power views (4×). The same areas were analysed for axonal pathology in the Bielschowsky silver stainings. Semi-quantitative analysis was performed as previously published.<sup>31</sup> In brief, axonal injury was established as follows: 0 = normal tissue; 1 = a few scattered injured axons; 2 = focused (up to 25% of a ×10 magnified field area) mild to moderate axonal injury; 3 = scattered mild to moderate or focused severe axonal injury; and 4 = scattered severe axonal injury. Axonal loss was determined using the following scale: 0, normal axonal density; 1 = focused mild to moderate axonal loss; 2 = scattered mild to moderate axonal loss; 3 = focused severe axonal loss; and 4 = scattered severe axonal loss. For each animal included in the analysis, an average of four sections from the brain and spinal cord (cervicothoracic and lumbosacral levels) were evaluated by a Board-certified veterinary pathologist (M.E.C.).

### Expansion and culture of human T cells

Human Th1 and Th17 lymphocytes were expanded and cultured as described previously.<sup>7</sup> Human CD14<sup>+</sup> monocytes and CD4<sup>+</sup>CD45RO<sup>+</sup> effector memory T cells were isolated from peripheral blood mononuclear cells of healthy donors using magnetic cell sorting (Miltenyi Biotec). Effector memory T cells (10<sup>6</sup>) cells were stimulated with anti-CD3 (2.5 µg/ml) cultured with autologous monocytes at a 5:3 ratio in X-VIVO<sup>TM</sup> 10 medium (Lonza) containing 5% human serum and 0.2% Normocure<sup>TM</sup>. For Th1 expansion, T lymphocytes were cultured in the presence of recombinant human interleukin (IL)-12 (10 ng/ml) and neutralizing antibody against IL-4 (5 µg/ml). For Th17 expansion, T lymphocytes were cultured in the presence of recombinant human IL-23 (25 ng/ml) and neutralizing antibodies against interferon (IFN)-γ (5 µg/ml) and against IL-4 (5 µg/ml). All antibodies and recombinant human proteins were purchased from BioLegend. To activate the Hh pathway, recombinant human SHH (100 ng/ml, R&D) was used at Days 0, 2 and 4. After 5 days of culture, cells were stimulated with phorbol 12-myristate 13-acetate (1 µg/ml, Sigma), ionomycin (20 ng/ml, Sigma) and brefeldin-A (5 µg/ml, BioLegend) for 4 h at 37°C and then stained for flow cytometry. For the proliferation assay, total human CD4 T cells were isolated from peripheral blood mononuclear cells of healthy donors, stained with 2 µM CFSE (BioLegend) according to the manufacturer's protocol and cultured for 5 days.

### 3' Digital gene expression sequencing

CD3<sup>+</sup>CD4<sup>+</sup>CD25<sup>+</sup>CD44<sup>+</sup>CD62L<sup>low</sup> cells were collected from the CNS of wild-type (*n* = 5) and CD4<sup>Cre</sup>Smo<sup>c/c</sup> (*n* = 6) mice at the peak of disease by flow sorting (Supplementary material). Total RNA was purified using the RNeasy<sup>®</sup> Plus microkit (Qiagen). An mRNA library was prepared using the SMART-Seq<sup>®</sup> HT kit (Clontech). Illumina indexes were added to cDNA using the Nextera XT DNA library preparation kit (Illumina). RNA-seq libraries were subjected to single end 75 bp read sequencing on an Illumina NextSeq 500 sequencer. Bioinformatic processing and analysis is detailed in the Supplementary material.

### Statistical analyses

Data were analysed using GraphPad Prism v.8 software. The Mann-Whitney test was used to compare flow cytometry and histological data from experimental groups. Two-way ANOVA was used to compare EAE scores between mice groups. Survival curves were compared with the log-rank test. Proportions of classical and atypical EAE were compared with the Fisher exact test. For *in vitro* differentiation assays, the paired-analysis Wilcoxon test was performed to analyse treated versus non-treated groups. Outliers

were identified and removed using the robust regression and outlier removal (ROUT) method. Statistics for transcriptomic analyses are detailed in the Supplementary material. Two-sided tests were used and P-values <0.05 were considered significant with \*P ≤ 0.05, \*\*P ≤ 0.01, \*\*\*P ≤ 0.001 and \*\*\*\*P ≤ 0.0001.

### Data availability

All data will be available upon reasonable request to any qualified researcher.

## Results

### Hh signalling deficiency in CD4 T cells exacerbates clinical and neuropathological features of EAE

To investigate the ability of the Hh pathway to directly modulate T cell-mediated responses during neuroinflammation, we generated a conditional knockout mouse in which the Hh signalling transducer smoothed (SMO) is specifically ablated in CD4 T cells (CD4<sup>Cre</sup>Smo<sup>c/c</sup>) (Supplementary Fig. 1A). Naïve animals showed no overt pathological phenotype up to ~12 months of age and no differences in leucocyte numbers in various immune organs under homeostasis, compared with the littermate controls (Supplementary Fig. 1B–E). Likewise, we did not detect any alteration in blood–brain barrier function and properties under homeostasis when SMO was abrogated in CD4 T cells (Supplementary Fig. 2). To assess the *in vivo* function of Hh signalling in CD4 T cells infiltrating the CNS, we induced active EAE in CD4<sup>Cre</sup>Smo<sup>c/c</sup> mice and wild-type. Hh signalling deficiency in CD4 T cells significantly exacerbated EAE without delaying its onset and increased disease incidence and mortality (Fig. 1A–C). Consistent with these findings, CD4<sup>Cre</sup>Smo<sup>c/c</sup> mice showed significant weight loss as compared to the wild-type (Supplementary Fig. 3A). The maximum disease score was higher in CD4<sup>Cre</sup>Smo<sup>c/c</sup> than wild-type mice (Fig. 1D) but did not differ between the two groups when only sick animals were included in the analysis (Supplementary Fig. 3B). Nevertheless, symptomatic CD4<sup>Cre</sup>Smo<sup>c/c</sup> mice presented an overall more severe disease course than sick wild-type mice (Supplementary Fig. 3C). Interestingly, a higher percentage of CD4<sup>Cre</sup>Smo<sup>c/c</sup> mice exhibited symptoms of atypical EAE characterized by prominent ataxia with spinning, compared with the wild-type (Fig. 1E). Altogether, these findings indicate that the absence of Hh signalling within the CD4 T cell compartment worsens the clinical signs of EAE.

We then determined the consequences of perturbing SHH signalling in CD4 T cells on key pathological hallmarks of multiple sclerosis/EAE plaques. Because of the difference in EAE incidence between CD4<sup>Cre</sup>Smo<sup>c/c</sup> and wild-type mice, we performed histological analyses only on symptomatic mice at the peak of disease. Demyelination and axonal loss were more prominent in CD4<sup>Cre</sup>Smo<sup>c/c</sup> mice (Fig. 1F). In active EAE, leucocyte infiltration normally occurs in the spinal cord, cerebellum and leptomeningeal spaces, yet CD4<sup>Cre</sup>Smo<sup>c/c</sup> mice exhibited exacerbated perivascular cuffing and parenchymal infiltration in areas normally unaffected by disease, including the external capsule (Fig. 1F), the striatum, thalamus and midbrain. We also found an increased frequency of immune cell infiltrates in the brain of CD4<sup>Cre</sup>Smo<sup>c/c</sup> mice (Fig. 1G). As infiltration of highly inflammatory leucocytes is often associated with blood–brain barrier dysfunction,<sup>10,32</sup> we studied parameters evocative of CNS vascular activation and disruption. We noted heightened expression levels of VCAM1 combined with extensive extravasation of the endogenous serum protein fibrinogen in CD4<sup>Cre</sup>Smo<sup>c/c</sup> animals (Fig. 1H–J). The enhanced blood–brain barrier permeability observed in CD4<sup>Cre</sup>Smo<sup>c/c</sup> EAE mice appears to be an

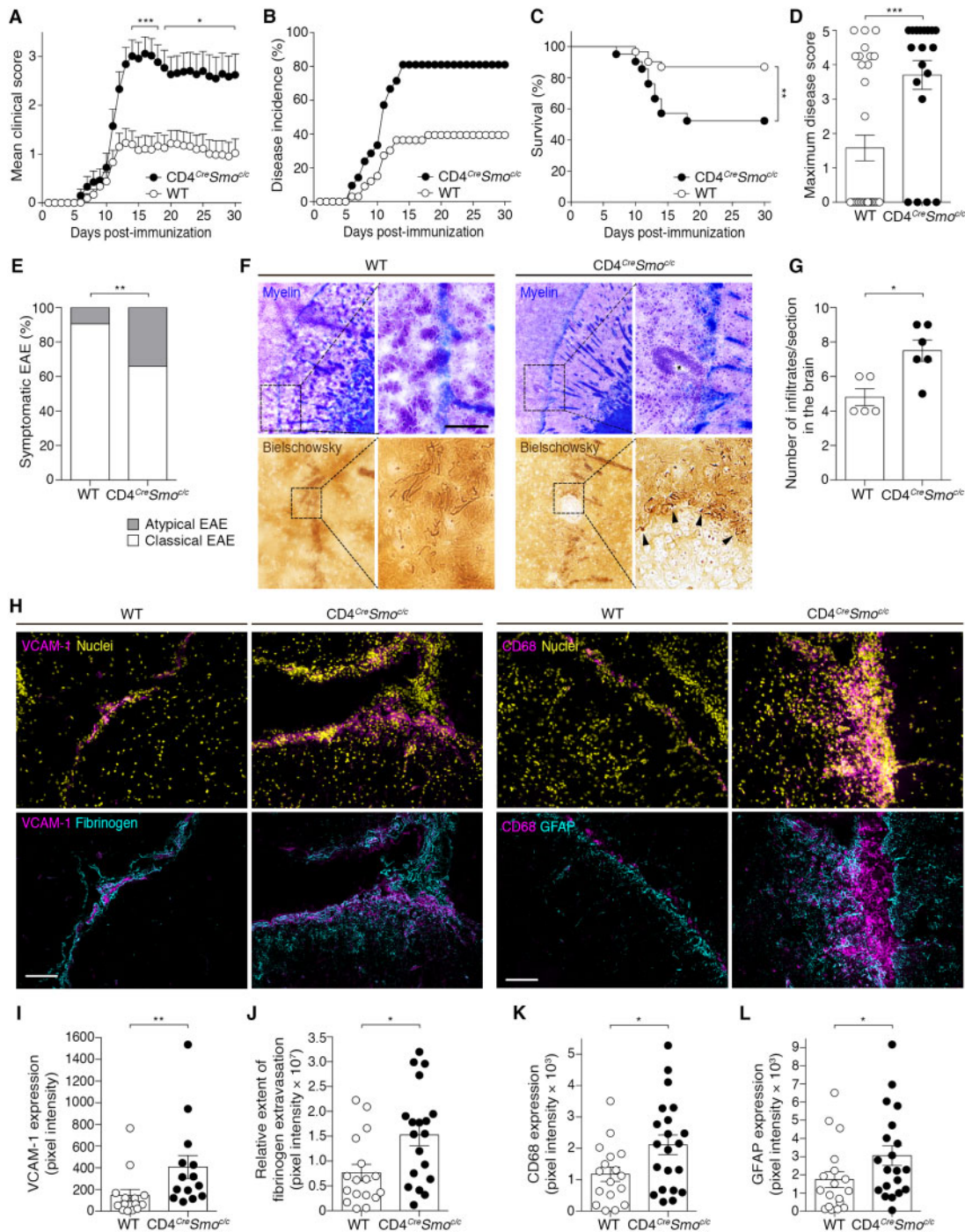


**Figure 1** Hh signalling deficiency in CD4 T cells exacerbates clinical and neuropathological features of EAE. (A) Cumulative clinical EAE score (mean  $\pm$  SEM), (B) disease incidence, (C) survival rate, (D) maximum disease score and (E) atypical and classical EAE presentation in MOG<sub>35-55</sub>-immunized CD4<sup>Cre</sup>Smo<sup>c/c</sup> mice and wild-type (WT) littermate controls. Data are representative of  $n = 30$  mice per genotype from three independent experiments. (F) Representative images depicting the extent of demyelination, immune cell infiltration (Luxol fast blue-haematoxylin and eosin staining; myelin: blue; cells: purple) and axonal damage (Bielschowsky's silver staining of nerve fibres) in the brain of CD4<sup>Cre</sup>Smo<sup>c/c</sup> and wild-type mice at the peak of disease. Scale bar = 100  $\mu$ m. (G) Quantification of the number of infiltrates per section and (H) immunofluorescent staining for VCAM1, CD68<sup>+</sup> macrophages/microglia (magenta), nuclei (DAPI, yellow), fibrinogen and GFAP (cyan) in the brain of CD4<sup>Cre</sup>Smo<sup>c/c</sup> and wild-type mice at the peak of EAE. Scale bars = 100  $\mu$ m. Images are representative of three meningeal infiltrates in  $n = 5$  (wild-type) and  $n = 6$  (CD4<sup>Cre</sup>Smo<sup>c/c</sup>) mice. (I–L) Quantification of (I) VCAM1, (J) fibrinogen leakage, (K) CD68 and (L) GFAP expression (mean  $\pm$  SEM of pixel intensity). (A) Two-way ANOVA with Sidak's correction for multiple comparisons. (C) Kaplan-Meier curves were compared using the Log-rank test. (D, G and I–L) Two-tailed Mann-Whitney test. (E) Fischer's exact test. \* $P \leq 0.05$ , \*\* $P \leq 0.01$  and \*\*\* $P \leq 0.001$ .

underlying consequence of the more severe disease course in these mice, rather than a direct effect of the mutation on baseline blood-brain barrier properties, as no differences in barrier integrity were

detected between wild-type and CD4<sup>Cre</sup>Smo<sup>c/c</sup> mice in an unchallenged state (Supplementary Fig. 2). The neuropathology of CD4<sup>Cre</sup>Smo<sup>c/c</sup> mice was also marked by increased astrogliosis and accumulation of CD68<sup>+</sup>

microglia/macrophages, particularly in heavily infiltrated meningeal and parenchymal areas (Fig. 1H, K and L). Furthermore, we detected a higher percentage of CD45<sup>hi</sup>CD11b<sup>+</sup>Ly6C<sup>hi</sup>Ly6G<sup>+</sup> inflammatory monocytes in the CNS of CD4<sup>Cre</sup>Smo<sup>c/c</sup> mice (Supplementary Fig. 3D), which is reported to correlate with EAE severity.<sup>33</sup>

### SMO deficiency promotes diffuse infiltration of CD4 T cells into the parenchyma during the course of EAE

As T cells play a key role in driving neuroinflammation in multiple sclerosis and EAE, we hypothesized that blocking Hh signalling in CD4 T cells could influence their infiltration and/or distribution within the CNS during disease. Surprisingly, the absolute number of CD4 T cells infiltrating the CNS of CD4<sup>Cre</sup>Smo<sup>c/c</sup> and wild-type mice at the peak of EAE were similar (Fig. 2A). However, in control

mice, these cells were predominantly located in close proximity to the CNS vasculature, including within leptomeningeal areas, whereas, in CD4<sup>Cre</sup>Smo<sup>c/c</sup> mice we detected a significant increase in the number of CD4<sup>+</sup> T cells diffusing throughout the parenchyma (Fig. 2B and C). Together, these findings indicate that inhibiting Hh signalling in CD4 T cells allows them to penetrate deeper into the parenchymal tissue instead of remaining confined to the perivascular space.

### Shh antagonizes the inflammatory program of CD4 T cells

Next, we determined whether SMO deficiency in CD4 T cells could alter their immunopathological response within the inflamed CNS. We found that, consistent with their more severe disease state,

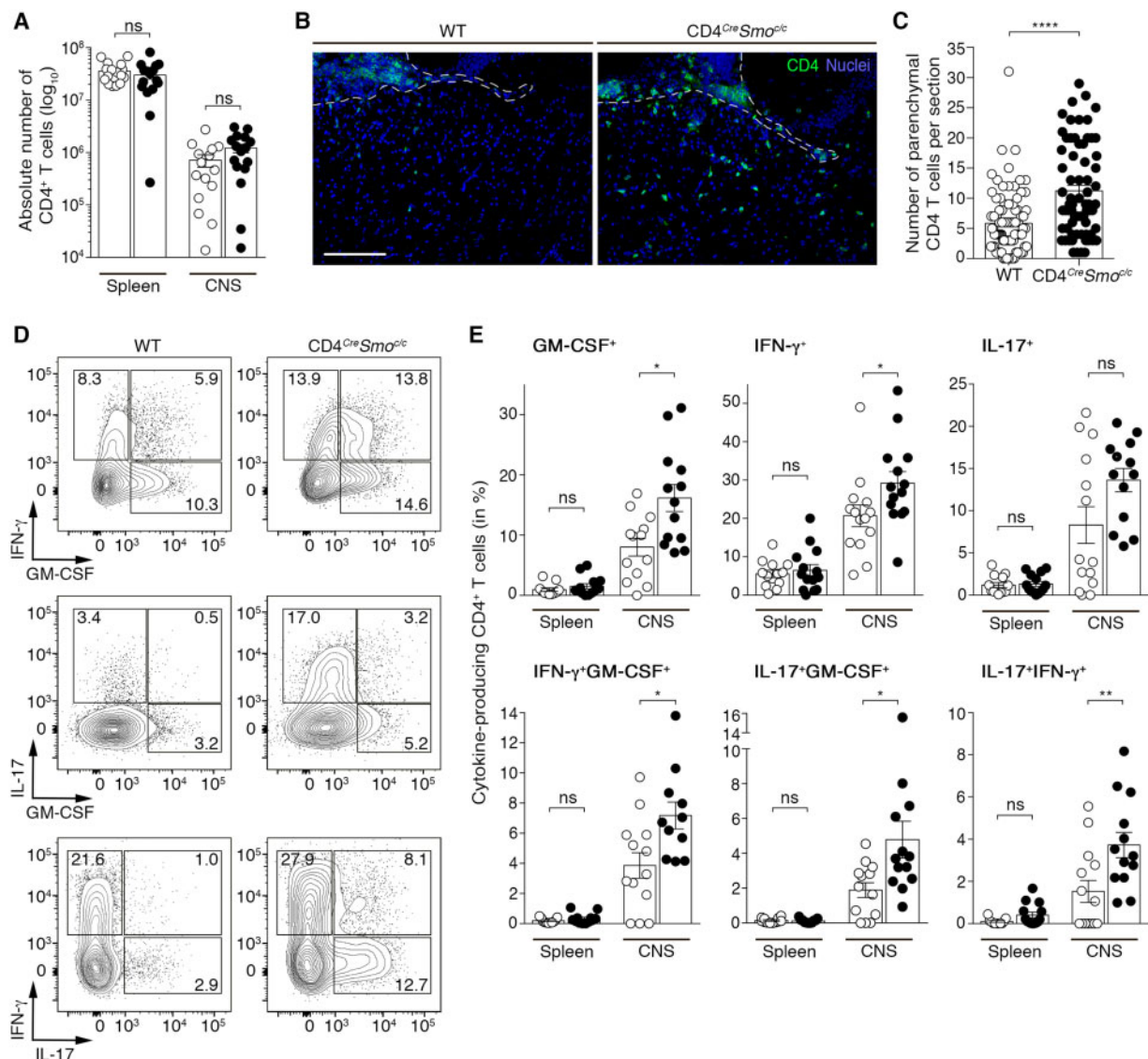


**Figure 2 SHH dampens the pathogenicity of CNS-infiltrating CD4 T cells.** (A) Absolute count of CD4<sup>+</sup> T lymphocytes in the spleen and CNS of wild-type (WT, open circles) and CD4<sup>Cre</sup>Smo<sup>c/c</sup> (filled circles) mice at the peak of EAE as assessed by flow cytometry. Data are expressed as means ± SEM and represent *n* = 6 independent experiments with five animals/group. (B) Immunofluorescent staining for CD4 (green) and nuclei (DAPI, blue) in the brain of CD4<sup>Cre</sup>Smo<sup>c/c</sup> and wild-type mice at the peak of disease. Dashed lines delineate the meninges bordering the brain parenchyma. Scale bar = 100 μm. (C) Quantification of 12 sections taken out of *n* = 5 wild-type and *n* = 6 CD4<sup>Cre</sup>Smo<sup>c/c</sup> animals. (D) Representative flow cytometry plots and (E) percentages of GM-CSF, IFN-γ, IL-17 single or double producing CD4 T cells in the spleen and CNS of wild-type (open circles) and CD4<sup>Cre</sup>Smo<sup>c/c</sup> (filled circles) mice at the peak of EAE. Data are representative of *n* = 6 independent experiments with 13–14 animals/group. (A, C and E) Two-tailed Mann-Whitney test. \*P < 0.05, \*\*P < 0.01 and \*\*\*\*P < 0.0001.

CD4<sup>Cre</sup>Smo<sup>c/c</sup> mice had significantly higher frequencies of CD4 T cells expressing the proinflammatory cytokines granulocyte-macrophage colony-stimulating factor (GM-CSF), IFN- $\gamma$  and IL-17 within the CNS at the peak of disease than wild-type mice (Fig. 2D and E). More importantly, we noted elevated numbers of T cells simultaneously producing a combination of the aforementioned cytokines in the CNS of CD4<sup>Cre</sup>Smo<sup>c/c</sup> mice (Fig. 2D and E). These T-cell subsets were shown to have a greater immunopathogenic potential in multiple sclerosis and EAE than single cytokine producers.<sup>7,34,35</sup> Notably, this effect was restricted to the CNS, as the production of pro-inflammatory mediators by CD4 T cells in the spleen was unaffected (Fig. 2E). To ascertain that the increased neuroinflammatory response seen in CD4<sup>Cre</sup>Smo<sup>c/c</sup>

mice is not the result of inherent differences in Th cell priming and differentiation, we isolated naïve CD4 T cells from the spleen of non-immunized wild-type and CD4<sup>Cre</sup>Smo<sup>c/c</sup> mice and polarized them *in vitro* into Th1 and Th17 cells. We found that Smo deletion in CD4 T cells did not affect their differentiation into the Th1 (Supplementary Fig. 4A–C) or the Th17 (Supplementary Fig. 4D–F) phenotype. Since the Hh pathway was reported to modulate T-cell receptor activation,<sup>18</sup> we interrogated antigen-specific responses in myelin oligodendrocyte glycoprotein (MOG)<sub>35–55</sub>-immunized CD4<sup>Cre</sup>Smo<sup>c/c</sup> mice and their littermate controls. We harvested the inguinal lymph nodes of wild-type and CD4<sup>Cre</sup>Smo<sup>c/c</sup> mice 12 days post-immunization, and purified CD4 T cells were cultured in the presence of MOG<sub>35–55</sub> peptide. SMO

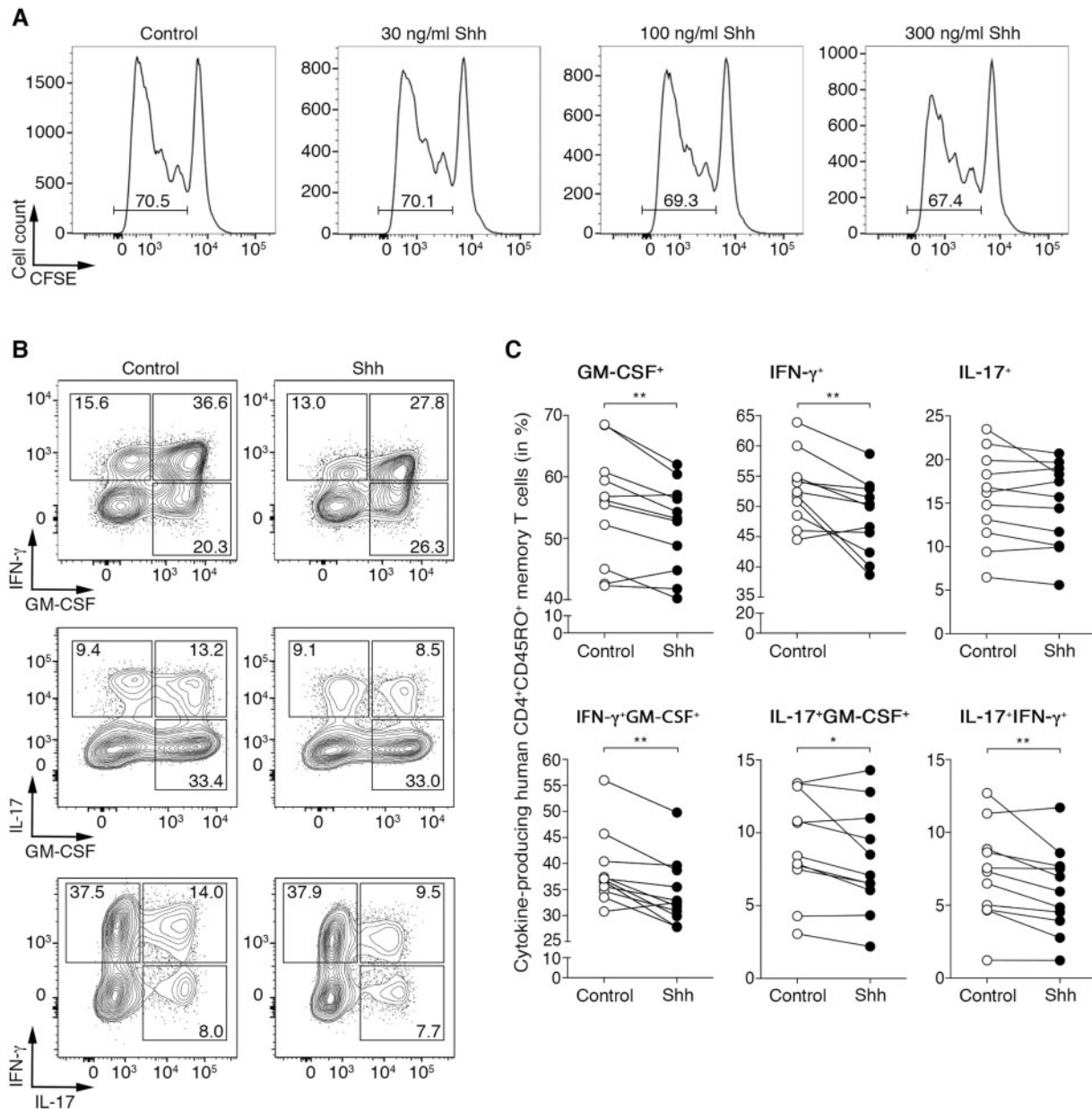


**Figure 3** SHH attenuates the pro-inflammatory phenotype of human memory CD4 T cells. (A) CFSE-labelled human CD4 T cells were cultured with anti-CD3/CD28 in the absence (control) or presence of the indicated doses of recombinant human SHH. Proliferation was determined after 5 days by flow cytometry. Data shown are representative of two independent experiments. (B and C) Human CD4<sup>+</sup>CD45RO<sup>+</sup> memory T cells isolated from the blood of healthy donors were cultured for 5 days under Th1-skewing conditions in the absence (control) or presence of 100 ng/ml recombinant human SHH. GM-CSF, IFN- $\gamma$  and IL-17 production was assessed in memory CD4 T cells by flow cytometry. (B) Representative dot plots are from  $n = 11$  donors and six independent experiments. (C) Each pair represents one donor stimulated without (control, open circles) or with (filled circles) recombinant human SHH. Wilcoxon test was used for comparisons. \* $P \leq 0.05$  and \*\* $P \leq 0.01$ .

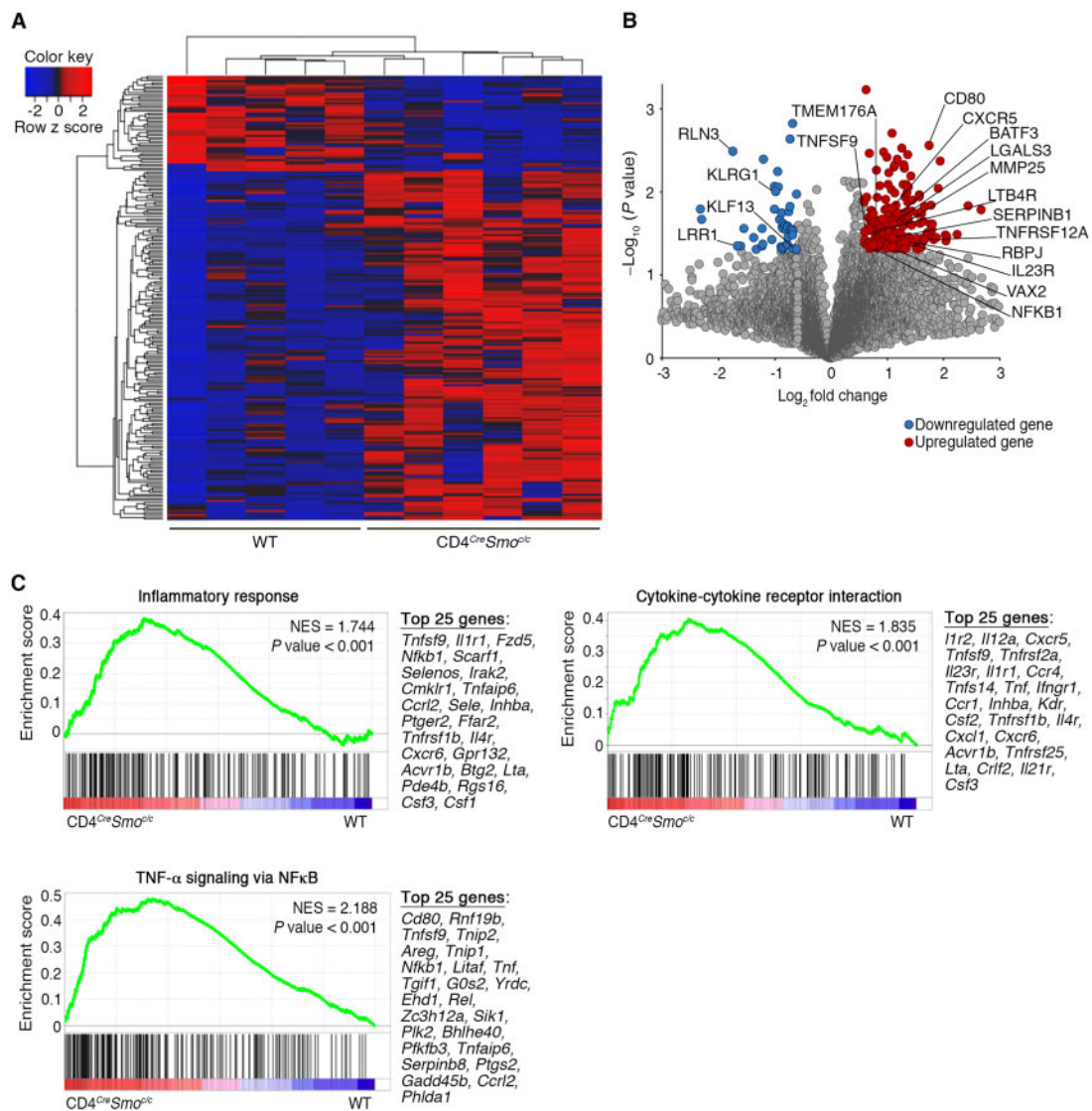


**Figure 4** The absence of Hh signalling in CD4 T cells promotes a pro-inflammatory transcriptomic profile in T cells infiltrating the CNS of EAE mice. (A) Heat map and (B) volcano plot of significantly differentially-expressed genes in flow-sorted CD3<sup>+</sup> CD4<sup>+</sup> CD25<sup>-</sup> CD44<sup>+</sup> CD62L<sup>low</sup> effector memory T cells from the CNS of wild-type (WT) (n = 5) and CD4<sup>Cre</sup>Smo<sup>-/-</sup> (n = 6) EAE mice at the peak of disease. Differentially expressed genes with an average fold change > 1.5 and P < 0.05 were considered significant. The 173 upregulated genes are shown in red and 47 downregulated genes in blue. (C and D) Gene set enrichment analysis of memory CD4 T cells invading the CNS of CD4<sup>Cre</sup>Smo<sup>-/-</sup> versus wild-type mice. (C) Representative gene set enrichment analysis plots of significantly enriched pathways associated with immune responses and ranked list of the 25 most-contributing genes (NES = normalized enrichment score; see also Table 1). Multiple t-tests were used for differential gene expression analyses in A and B. Gene sets with both a P-value < 0.05 and false discovery rate (FDR) < 0.05 for hallmark gene sets and recommended FDR < 0.25 for the C2 gene set enrichment analysis MSigDB compendium were considered significant (C and Table 1).

deficiency in CD4 T cells did not affect the proliferation rate of MOG<sub>35-55</sub>-specific T cells (Supplementary Fig. 4G and H) or their immune phenotype (Supplementary Fig. 4I and J). Thus, during EAE, Hh deficiency within CD4 T cells does not alter MOG-specific activation and proliferation in the periphery, confirming the CNS-centric effect of the Hh pathway in pathological neuroinflammation.

To emulate the effect of Shh on T cells infiltrating the inflamed multiple sclerosis brain, CD4<sup>+</sup> CD45RO<sup>+</sup> memory T cells isolated from the peripheral blood of healthy donors were skewed into the Th1 or Th17 phenotype in the presence or absence of recombinant Shh. We used memory effector (rather than CD45RA<sup>+</sup> naive) T cells, as they are the ones that cross the blood–brain barrier and get reactivated within the CNS to drive multiple sclerosis and EAE disease pathology.<sup>32,36,37</sup> First, we found that none of the SHH concentrations tested impacted T-cell proliferation (Fig. 3A). However, SHH (100 ng/

ml) reduced GM-CSF and IFN-γ expression and the frequencies of IFN-γ<sup>+</sup> GM-CSF<sup>+</sup>, IL-17<sup>+</sup> GM-CSF<sup>+</sup> and IFN-γ<sup>+</sup> IL-17<sup>+</sup> double producers in human Th1-cultured cells only, while IL-17 production remained unaffected (Fig. 3B and C). In contrast, no significant changes were detected in the inflammatory phenotype of Th17 cells cultured in the presence of SHH (Supplementary Fig. 5). These data corroborate our findings in mice and confirm a key role for the Hh pathway in attenuating the inflammatory status of Th cells.

### The absence of Hh signalling promotes a pro-inflammatory transcriptomic profile in CNS-invading CD4 T cells

To gain further insight into the mechanisms that contribute to the enhanced pathogenic profile of SMO-deficient T cells,



we performed a bulk transcriptomic analysis of CD3<sup>+</sup>CD4<sup>+</sup>CD44<sup>+</sup>CD62L<sup>low</sup>CD25<sup>−</sup> memory T cells isolated from the CNS of CD4<sup>CreSmo<sup>c/c</sup></sup> and wild-type EAE mice at the peak of disease. Unbiased analysis showed a significant genotype-based clustering of 220 genes, underlying a unique signature driven by SMO-dependent Hh signalling in memory T cells infiltrating the CNS (Fig. 4A and B). Among these differentially expressed genes, 173 are upregulated in CD4<sup>CreSmo<sup>c/c</sup></sup> and 47 in wild-type mice (Fig. 4B and Supplementary Table 1). Specifically, we observed an upregulation of SerpinB1, the leukotriene B4 receptor (*Ltb4r*), galectin-3 (*Lgals3*) and *Tnfrsf9* (CD137L), genes that were all shown to exacerbate EAE by driving Th1 and Th17 immune responses<sup>38–42</sup>. Similarly, we report high expression of several Th17 lineage-associated genes, including *Il23r*, *Rbpj*,<sup>43</sup> *Batf3*,<sup>44</sup> *Nr1d1* (REV-ERB $\alpha$ ) and *Nr1d2* (REV-ERB $\beta$ ),<sup>45</sup> *Vax2*, *Tmem176a* and *Ltb4r*.<sup>46</sup> Interestingly, downregulated genes in memory CD4 T cells from CD4<sup>CreSmo<sup>c/c</sup></sup> mice comprise *Klrg1*, a co-inhibitory receptor for T cells,<sup>47</sup> and *Rh3*, which is reported to decrease GM-CSF and IL-6 production<sup>48</sup> (Fig. 4A and B, and Supplementary Table 1).

Significantly enriched pathways in memory CD4 T cells from CD4<sup>CreSmo<sup>c/c</sup></sup> mice are primarily associated with inflammatory responses (Fig. 4C, Table 1, Supplementary Fig. 6 and Supplementary Table 2). Leading-edge analysis shows that within the hallmark ‘TNF $\alpha$  signalling via NF- $\kappa$ B’ and ‘inflammatory response’, as well as the ‘cytokine-cytokine receptor interaction’ KEGG gene sets, the genes primarily contributing to this effect include inflammatory cytokines and chemokine receptors involved in T cell-mediated neuroinflammation<sup>49,50</sup> (Fig. 4C, Table 1 and Supplementary Fig. 6).

Gene sets related to the NF- $\kappa$ B pathway and TNF $\alpha$ -associated genes are also highly enriched in CNS-infiltrating T cells of CD4<sup>CreSmo<sup>c/c</sup></sup> mice (Fig. 4C, Table 1, Supplementary Fig. 6, Supplementary Tables 1 and 2). In keeping with our clinical, immunological and pathological findings, these analyses reveal that the lack of Hh signalling renders CD4 memory T cells more encephalitogenic by inducing a shift towards an inflammatory transcriptional profile.

### In vivo therapeutic treatment with an Hh pathway agonist alleviates CD4 T cell-driven neuroinflammation

Our findings underscore an important neuroprotective role for Hh signalling during EAE through modulation of the inflammatory phenotype of CD4 T cells. Thus, we investigated whether therapeutic treatment with an agonist of the Hh pathway could be used as intervention to dampen ongoing CD4 T cell-driven

neuroinflammation in wild-type mice. We used a synthetic SMO agonist previously described to activate the Hh pathway<sup>51</sup> and capable of reaching the CNS.<sup>52,53</sup> Animals were monitored twice a day for the development of clinical signs of EAE and upon disease onset received one daily intraperitoneal injection of 20  $\mu$ g/g SMO agonist for three consecutive days. Treatment of EAE mice with the SMO agonist stabilized the clinical course of the disease, preventing worsening of paralysis and ataxia and significantly improved survival, compared with vehicle-injected controls (Fig. 5A, B and Supplementary Movies 1 and 2). Of note, the mortality rate of control wild-type EAE mice in this set of experiments was higher than the one described earlier (Fig. 1C), as only sick mice with a score of  $\geq 1.5$  at onset were considered. Stabilization of the disease in SMO agonist-treated mice correlated with decreased percentages of GM-CSF<sup>+</sup> and IFN- $\gamma$ <sup>+</sup> GM-CSF<sup>+</sup> CNS-infiltrating CD4 T cells (Fig. 5C and D). SMO-agonism significantly dampened inflammation and demyelination (Fig. 5E–G), as well as axonal blebbing in the spinal cord, brainstem and cerebellum (Fig. 5H–J). In vehicle-treated mice with cerebellar disease involvement, we observed axonal torpedoes within the granular layer and loss of Purkinje cells with surrounding hairy baskets that were significantly reduced in SMO agonist-treated mice (Fig. 5H and J). Thus, therapeutic treatment with an agonist of the Hh pathway improves the clinical and neuropathological signs of EAE, at least in part by attenuating inflammatory T-cell responses within the CNS compartment.

## Discussion

In EAE, and presumably in multiple sclerosis, the majority of CNS-infiltrating CD4 T cells acquire an aggressive Th1-like phenotype and become IFN- $\gamma$  and GM-CSF producers within the inflamed CNS.<sup>34,54,55</sup> These Th cells, particularly the ones characterized by the coordinated expression of two or more inflammatory cytokines, are considered essential mediators of disease in mice and humans.<sup>10,56–58</sup> Their recruitment and accumulation within the CNS trigger an inflammatory cascade causing tissue damage and the formation of multiple sclerosis/EAE lesions. Successful resolution of neuroinflammation depends upon clearance of these cells or at minimum reducing their pathogenic activity to prevent the development of persistent chronic inflammation. Earlier studies have shown that SHH, whose expression is considerably upregulated by astrocytes in multiple sclerosis and EAE lesions, promotes blood–brain barrier integrity.<sup>10,11,59</sup> Now we show that Hh signalling facilitates the return to tissue homeostasis by

**Table 1** List of gene sets positively and negatively enriched in CNS-invading CD4 T cells

Gene set	Normalized enrichment score	P-value
TNF $\alpha$ signalling via NF- $\kappa$ B	2.188	<0.001
KRAS signalling	1.876	<0.001
NOTCH1 intracellular domain regulates transcription	1.871	0.001
Nuclear receptor transcription pathway	1.844	0.001
Cytokine-cytokine receptor interaction	1.811	<0.001
TNF receptor superfamily TNFSF members mediating non-canonical NF- $\kappa$ B pathway	1.800	0.003
IL-2/STAT-5 signalling	1.770	<0.001
Type I diabetes mellitus	1.744	0.001
Inflammatory response	1.744	<0.001
TGF $\beta$ signalling	1.692	0.004
Hypoxia	1.639	<0.001
p53 pathway	1.602	0.001
IL-6/JAK/STAT-3 signalling	1.548	0.012
E2F targets	−1.583	<0.001
Minichromosome maintenance pathway	−2.051	<0.001

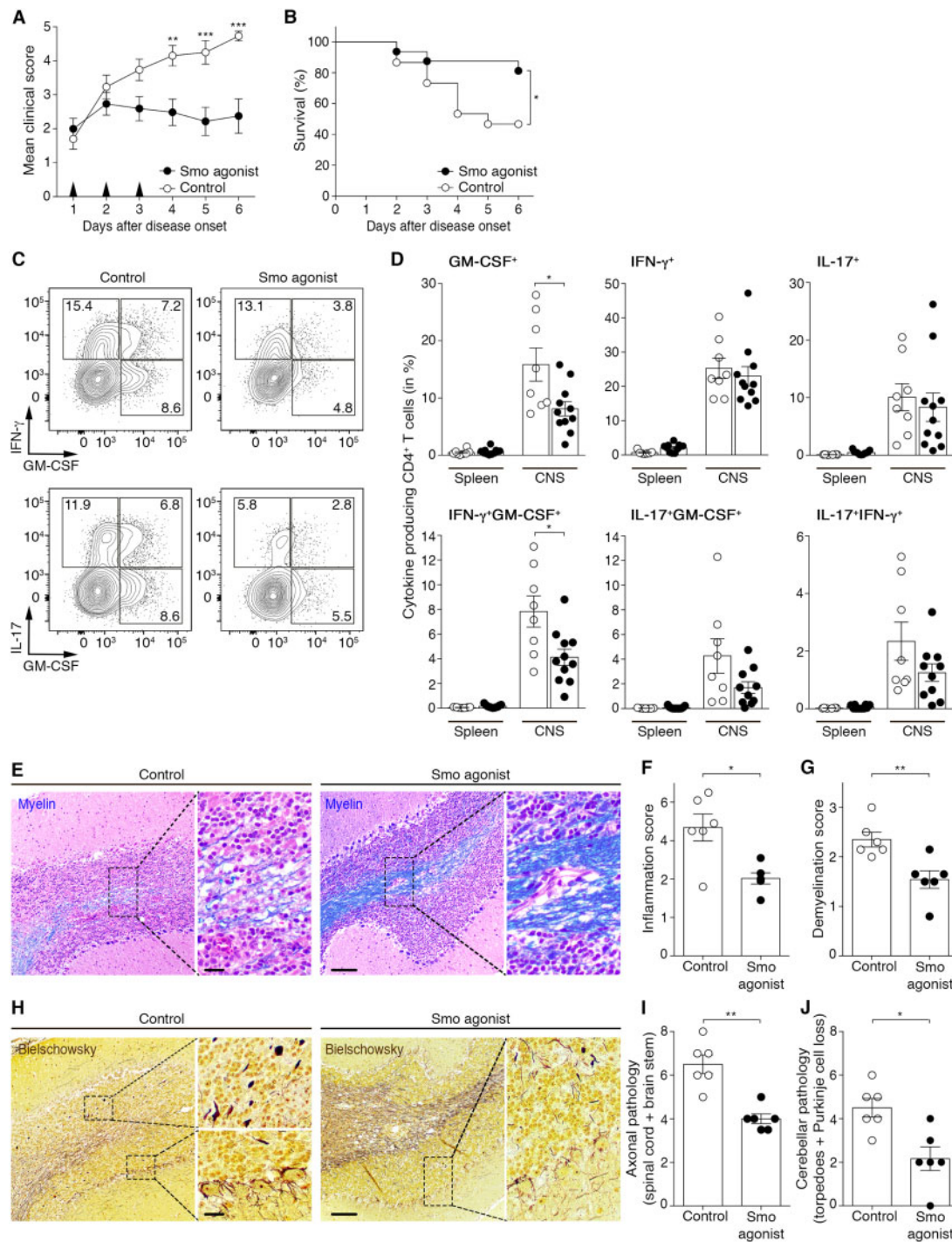


**Figure 5** *In vivo* therapeutic treatment with an agonist of the Hh pathway alleviates CD4 T cell-driven neuroinflammation. (A) Cumulative clinical EAE score (mean ± SEM) and (B) survival rate of MOG<sub>35-55</sub>-immunized wild-type (WT) mice treated with vehicle control or SMO agonist for three consecutive days following disease onset. Data shown are from *n* = 15 controls and *n* = 16 SMO agonist-treated mice and four independent experiments. (C) Representative flow cytometry plots and (D) percentages of GM-CSF, IFN- $\gamma$  and IL-17 single and dual-producing CD4 T cells isolated from the spleen and CNS of vehicle control (open circles)- or SMO agonist (filled circles)-treated mice 6 days post-disease onset. Data are from *n* = 8 controls and *n* = 11 SMO agonist-treated mice from four independent experiments. (E) Representative images depicting the extent of demyelination [Luxol fast blue/haematoxylin/eosin staining; myelin (blue) and nuclei (purple)] in control- and SMO agonist-treated mice at Day 6 post-disease onset. Scale bar = 100  $\mu$ m. (F and G) Inflammation and demyelination scores in the CNS of *n* = 6 controls and *n* = 6 SMO agonist-treated mice. (H) Representative images showing axonal damage (Bielschowsky's silver staining) in the brain of vehicle control- or SMO agonist-treated mice 6 days after EAE onset. Scale bars = 20  $\mu$ m and 100  $\mu$ m. (I) Axonal pathology score in the brainstem and spinal cord and (J) in the cerebellum of *n* = 6 controls and *n* = 6 SMO agonist-treated mice. (A) Two-way ANOVA with Sidak's correction for multiple comparisons. (B) Kaplan-Meier curves were compared using the Log-rank test. (D, F, G, I and J) Mann-Whitney test was used for comparisons. \**P* ≤ 0.05, \*\**P* ≤ 0.01 and \*\*\**P* ≤ 0.001.

directly modulating T cell immune responses within the CNS inflammatory milieu. We demonstrate, using a conditional knockout in which the Hh pathway is rendered inactive exclusively in CD4 T cells, that SMO-dependent Hh signalling diminishes the frequency of GM-CSF<sup>+</sup>IFN- $\gamma$ <sup>+</sup>, IFN- $\gamma$ <sup>+</sup>IL17<sup>+</sup> and GM-CSF<sup>+</sup>IL-17<sup>+</sup> CD4 T cells within the CNS compartment. In contrast, peripheral MOG-specific CD4 T-cell responses remain unaltered, compared with control mice. This CNS-centric effect is likely to be the result of exacerbated Shh production in the inflamed CNS, as seen in multiple sclerosis and EAE.<sup>10</sup> Similarly, site-specific modulation of the Hh pathway in inflamed tissues has recently been reported in a model of atopic dermatitis.<sup>22</sup> Likewise, in humans, the expansion of CD4<sup>+</sup>CD45RO<sup>+</sup> memory T cells in the presence of exogenous Shh decreases their expression of pro-inflammatory cytokines and the frequency of double producers, data that are in agreement with the reported modulation of human Th2 cytokines by Hh signalling *in vitro*.<sup>60</sup>

Amongst the pro-inflammatory cytokines produced by auto-reactive Th cells, GM-CSF is widely regarded as essential to the pathology of EAE<sup>34,35</sup> and multiple sclerosis.<sup>57,61</sup> Our study shows that the lack of Hh signalling in CD4 T cells replicates several features of GM-CSF-mediated neuroinflammation.<sup>62–66</sup> In particular, it causes CD4 T cells to invade the CNS parenchyma beyond the meningeal and perivascular space and supports the accumulation of CD68 macrophages/microglia and the recruitment of inflammatory Ly6C<sup>hi</sup> monocytes. It also increases leakiness and activation of the blood–brain barrier and promotes astrogliosis, reflecting the magnitude of the neuroinflammatory response driven by pathogenic T cells.<sup>67–69</sup> Clinically, *Smo* deletion in CD4 T cells increases the propensity of atypical ataxic EAE evoking predominant brain-cerebellum-brainstem inflammation,<sup>29</sup> dependent on the GM-CSF/IL-17 axis.<sup>30,70</sup> Conversely, we found a reduction in the percentages of GM-CSF<sup>+</sup> single and GM-CSF<sup>+</sup>IFN- $\gamma$ <sup>+</sup> double producers in wild-type animals treated with a SMO agonist after disease onset.

We interrogated at a more granular level the transcriptional program driven by SMO-dependent signalling in CD4 T cells and found that several genes known to promote T-cell pathogenicity in EAE are upregulated or enriched in the CNS of CD4<sup>Cre</sup>*Smo*<sup>c/c</sup> mice including *Rbpj*,<sup>43</sup> *Batf3*,<sup>71</sup> *SerpinB1*,<sup>38</sup> *Il23r*, *Cxcr4*, *Cxcr6* and *Il1r1*.<sup>72</sup> Compromised Hh signalling in CD4 T cells also promotes enrichment of the IL2/STAT5 signalling pathway. STAT-5 has emerged as an absolute requirement for Th pathogenicity by favouring the development of GM-CSF<sup>+</sup> T cells in EAE and multiple sclerosis.<sup>73,74</sup> It is worth mentioning as well that IL2RA and IL7RA share a common  $\gamma$ c chain and their polymorphisms are among the highest genetic risk factors for multiple sclerosis.<sup>75,76</sup> Also enriched in *Smo*-deficient CNS-invading CD4 T cells, the NF- $\kappa$ b pathway has been directly linked to T-cell pathogenicity in EAE, including through GM-CSF production<sup>77,78</sup> and by inducing rapid expression of TNF $\alpha$ , IL-1 $\beta$ , and IL-6.<sup>79</sup> Overall, a significant number of transcripts associated with inflammatory Th cell-fate, pro-inflammatory cytokines, and T-cell activation are enriched in CNS-infiltrating *Smo*-deficient CD4 T cells. Conversely, gene set enrichment analyses reveal enrichment of a few anti-inflammatory pathways in CD4<sup>Cre</sup>*Smo*<sup>c/c</sup> mice, such as transforming growth factor- $\beta$ ,<sup>80</sup> PDGF/RAS/RAF/MEK, PI3K/AKT/mTOR and Wnt signalling, which may reflect compensatory mechanisms to overcome neuroinflammation in the absence of Hh signalling.<sup>81</sup> Altogether, these findings underscore the essential role of SMO-dependent Hh signalling in CD4 T cells to limit neuroinflammation.

Corroborating these results, activation of the Hh signalling pathway by SMO agonism after the onset of EAE symptoms remarkably stabilizes the course of the disease and decreases mortality. The reduced pathogenicity of CD4 T cells following SMO agonist treatment correlates with decreased demyelination and

axonal damage in the brain, brainstem, cerebellum and spinal cord. Of note, immunological/pathological analyses were performed at the peak of disease, highlighting the essential regulatory role of the Hh pathway in containing acute neuroinflammation. Another interesting observation from our study is that SMO agonism therapy effectively alleviates both classical and atypical symptoms of EAE. Consistent with the latter, treatment with a SMO agonist appears protective against axonal damage in the granular layer and Purkinje cells of the cerebellum. Collectively, these clinical, immunological and histological findings show the beneficial effect of SMO agonism in controlling acute neuroinflammation, particularly the one mediated by GM-CSF-producing T cells. We did not observe any adverse side effects upon SMO agonist treatment for the duration of the study, in accordance with previous reports.<sup>53,82</sup> Nevertheless, CNS and non-CNS effects of SMO agonist treatment should be investigated further following prolonged exposure.

Herein, we provide evidence that the Hh signalling pathway, activated within the CNS as part of the host response during the inflammatory phase of multiple sclerosis and EAE, acts at the crosstalk between the CNS and the immune system to limit uncontrolled T-cell responses under the pathological state. We demonstrate its ability to attenuate the pathogenic profile of human and mouse effector Th cells by regulating their production of pro-inflammatory cytokines. From a therapeutic point of view, we show that systemic administration of a Hh agonist after the onset of EAE symptoms effectively halts disease progression and significantly reduces neuroinflammation and the underlying neuropathology, thus highlighting the potential benefit in exploiting this neuroimmune network as a strategy to antagonize ongoing neurological disease and promote the resolution of inflammation.

## Acknowledgements

We thank Dr Daniel Beiting and Megan Sullivan for their advice and technical support in preparing samples for RNA sequencing. We appreciate the advice from Dr Gordon Ruthel at the Penn Vet Imaging Core of the University of Pennsylvania and Drs Charles Vite and Gary Swain (Clinical Sciences and Advance Medicine—Penn Vet) for assistance on scoping and image analysis. We also thank Trini Ochoa for technical assistance in EAE experiments. We are indebted to ULAR personnel for animal care.

## Funding

The National Institutes of Health (NIH) of the United States has supported this work through the following grant NINDS 5K01NS097519-03 (J.I.A.). J.I.A. held the EndMS David L. Torrey TCD award from the Multiple Sclerosis Society of Canada (MSSC). N.B. is funded by Inserm and holds a scholarship from the Fulbright program and a travel grant from the Fondation pour l'Aide à la Recherche sur la Sclérose en Plaques (ARSEP). H.K. holds a postdoctoral fellowship award from the Fonds de Recherche du Québec-Santé (FRQS). M.S.A. is a Cancer Research Institute (CRI) Irvington Postdoctoral Fellow and is supported by the FRQS and Canadian Network on Hepatitis C (CanHepC) Postdoctoral Fellowships. CanHepC is funded by a joint initiative from CIHR (NHC-142832) and the Public Health Agency of Canada. C.L. holds a scholarship from the Chinese Scholarship Council (CSC) (201904910180).

## Competing interests

The authors report no competing interests.

## Supplementary material

Supplementary material is available at *Brain* online.

## References

- Lucchinetti C, Brück W, Parisi, J Scheithauer, B Rodriguez, M Lassmann, H. Heterogeneity of multiple sclerosis lesions: Implications for the pathogenesis of demyelination. *Ann Neurol*. 2000;47(6):707–717.
- Alvarez JI, Saint-Laurent O, Godschalk A, et al. Focal disturbances in the blood-brain barrier are associated with formation of neuroinflammatory lesions. *Neurobiol Dis*. 2015;74:14–24.
- Trapp BD, Peterson J, Ransohoff RM, Rudick R, Mörk S, Bö L. Axonal transection in the lesions of multiple sclerosis. *N Engl J Med*. 1998;338(5):278–285.
- Weiner HL. The challenge of multiple sclerosis: How do we cure a chronic heterogeneous disease? *Ann Neurol*. 2009;65(3):239–248.
- Brucklacher-Waldert V, Stuermer K, Kolster M, Wolthausen J, Tolosa E. Phenotypical and functional characterization of T helper 17 cells in multiple sclerosis. *Brain*. 2009;132(Pt 12):3329–3341.
- Johnson MC, Pierson ER, Spieker AJ, et al. Distinct T cell signatures define subsets of patients with multiple sclerosis. *Neurol Neuroimmunol Neuroinflamm*. 2016;3(5):e278.
- Kebir H, Ifergan I, Alvarez JI, et al. Preferential recruitment of interferon-gamma-expressing TH17 cells in multiple sclerosis. *Ann Neurol*. 2009;66(3):390–402.
- Miller AH, Haroon E, Felger JC. Therapeutic implications of brain-immune interactions: Treatment in translation. *Neuropsychopharmacol*. 2017;42(1):334–359.
- Prud'homme GJ, Glinka Y, Wang Q. Immunological GABAergic interactions and therapeutic applications in autoimmune diseases. *Autoimmun Rev*. 2015;14(11):1048–1056.
- Alvarez JI, Dodelet-Devillers A, Kebir H, et al. The hedgehog pathway promotes blood-brain barrier integrity and CNS immune quiescence. *Science*. 2011;334(6063):1727–1731.
- Podjaski C, Alvarez JI, Bourbonniere L, et al. Netrin 1 regulates blood-brain barrier function and neuroinflammation. *Brain*. 2015;138(Pt 6):1598–1612.
- Briscoe J, Therond PP. The mechanisms of hedgehog signalling and its roles in development and disease. *Nat Rev Mol Cell Biol*. 2013;14(7):416–429.
- Garcia ADR, Han YG, Triplett JW, Farmer WT, Harwell CC, Ihrle RA. The elegance of sonic hedgehog: Emerging novel functions for a classic morphogen. *J Neurosci*. 2018;38(44):9338–9345.
- Dellovade T, Romer JT, Curran T, Rubin LL. The hedgehog pathway and neurological disorders. *Annu Rev Neurosci*. 2006;29:539–563.
- Furmanski AL, Saldana JI, Rowbotham NJ, Ross SE, Crompton T. Role of hedgehog signalling at the transition from double-positive to single-positive thymocyte. *Eur J Immunol*. 2012;42(2):489–499.
- Outram SV, Varas A, Pepicelli CV, Crompton T. Hedgehog signaling regulates differentiation from double-negative to double-positive thymocyte. *Immunity*. 2000;13(2):187–197.
- Furmanski AL, Saldana JI, Ono M, et al. Tissue-derived hedgehog proteins modulate Th differentiation and disease. *J Immunol*. 2013;190(6):2641–2649.
- Rowbotham NJ, Hager-Theodorides AL, Cebecauer M, et al. Activation of the Hedgehog signaling pathway in T-lineage cells inhibits TCR repertoire selection in the thymus and peripheral T-cell activation. *Blood*. 2007;109(9):3757–3766.
- Kwon H, Song K, Han C, et al. Inhibition of hedgehog signaling ameliorates hepatic inflammation in mice with nonalcoholic fatty liver disease. *Hepatology*. 2016;63(4):1155–1169.
- Lee JJ, Rothenberg ME, Seeley ES, Zimdahl B, et al. Control of inflammation by stromal Hedgehog pathway activation restrains colitis. *Proc Natl Acad Sci U S A*. 2016;113(47):E7545–E7553.
- Michelotti GA, Xie G, Swiderska M, et al. Smoothed is a master regulator of adult liver repair. *J Clin Invest*. 2013;123(6):2380–2394.
- Papaioannou E, Yanez DC, Ross S, et al. Sonic hedgehog signaling limits atopic dermatitis via Gli2-driven immune regulation. *J Clin Invest*. 2019;129(8):3153–3170.
- Stewart GA, Hoyne GF, Ahmad SA, et al. Expression of the developmental Sonic hedgehog (Shh) signalling pathway is up-regulated in chronic lung fibrosis and the Shh receptor patched 1 is present in circulating T lymphocytes. *J Pathol*. 2003;199(4):488–495.
- Fan Q, He M, Sheng T, et al. Requirement of TGFbeta signaling for SMO-mediated carcinogenesis. *J Biol Chem*. 2010;285(47):36570–36576.
- Hanna A, Metge BJ, Bailey SK, et al. Inhibition of Hedgehog signaling reprograms the dysfunctional immune microenvironment in breast cancer. *Oncoimmunology*. 2019;8(3):1548241.
- Palma V, Lim DA, Dahmane N, et al. Sonic hedgehog controls stem cell behavior in the postnatal and adult brain. *Development*. 2005;132(2):335–344.
- Traiffort E, Angot E, Ruat M. Sonic hedgehog signaling in the mammalian brain. *J Neurochem*. 2010;113(3):576–590.
- Seifert T, Bauer J, Weissert R, Fazekas F, Storch MK. Differential expression of sonic hedgehog immunoreactivity during lesion evolution in autoimmune encephalomyelitis. *J Neuropathol Exper Neurol*. 2005;64(5):404–411.
- Muller DM, Pender MP, Greer JM. A neuropathological analysis of experimental autoimmune encephalomyelitis with predominant brain stem and cerebellar involvement and differences between active and passive induction. *Acta Neuropathol*. 2000;100(2):174–182.
- Spath S, Komuczki J, Hermann M, et al. Dysregulation of the cytokine GM-CSF induces spontaneous phagocyte invasion and immunopathology in the central nervous system. *Immunity*. 2017;46(2):245–260.
- Kassis I, Grigoriadis N, Gowda-Kurkalli B, et al. Neuroprotection and immunomodulation with mesenchymal stem cells in chronic experimental autoimmune encephalomyelitis. *Arch Neurol*. 2008;65(6):753–761.
- Kebir H, Kreyenborg K, Ifergan I, et al. Human TH17 lymphocytes promote blood-brain barrier disruption and central nervous system inflammation. *Nat Med*. 2007;13(10):1173–1175.
- Mildner A, Mack M, Schmidt H, et al. CCR2 + Ly-6Chi monocytes are crucial for the effector phase of autoimmunity in the central nervous system. *Brain*. 2009;132(Pt 9):2487–2500.
- Codarri L, Gyulveszi G, Tosevski V, et al. RORgammaT drives production of the cytokine GM-CSF in helper T cells, which is essential for the effector phase of autoimmune neuroinflammation. *Nat Immunol*. 2011;12(6):560–567.
- El-Behi M, Ciric B, Dai H, et al. The encephalitogenicity of T(H)17 cells is dependent on IL-1- and IL-23-induced production of the cytokine GM-CSF. *Nat Immunol*. 2011;12(6):568–575.
- Kivisakk P, Mahad DJ, Callahan MK, et al. Human cerebrospinal fluid central memory CD4+ T cells: Evidence for trafficking through choroid plexus and meninges via P-selectin. *Proc Natl Acad Sci U S A*. 2003;100(14):8389–8394.
- Schafflick D, Xu CA, Hartlehnert M, et al. Integrated single cell analysis of blood and cerebrospinal fluid leukocytes in multiple sclerosis. *Nat Commun*. 2020;11(1):247.

38. Hou L, Rao DA, Yuki K, et al. SerpinB1 controls encephalitogenic T helper cells in neuroinflammation. *Proc Natl Acad Sci U S A*. 2019;116(41):20635–20643.
39. Jiang HR, Al Rasebi Z, Mensah-Brown E, et al. Galectin-3 deficiency reduces the severity of experimental autoimmune encephalomyelitis. *J Immunol*. 2009;182(2):1167–1173.
40. Kihara Y, Yokomizo T, Kunita A, et al. The leukotriene B4 receptor, BLT1, is required for the induction of experimental autoimmune encephalomyelitis. *Biochem Biophys Res Commun*. 2010;394(3):673–678.
41. Martinez Gomez JM, Croxford JL, Yeo KP, Angeli V, Schwarz H, Gasser S. Development of experimental autoimmune encephalomyelitis critically depends on CD137 ligand signaling. *J Neurosci*. 2012;32(50):18246–18252.
42. Zhao P, Hou L, Farley K, Sundrud MS, Remold-O'Donnell E. SerpinB1 regulates homeostatic expansion of IL-17+ gamma-delta and CD4+ Th17 cells. *J Leukocyte Biol*. 2014;95(3):521–530.
43. Meyer Zu Horste G, Wu C, Wang C, et al. RBPJ controls development of pathogenic Th17 cells by regulating IL-23 receptor expression. *Cell Rep*. 2016;16(2):392–404.
44. Schraml BU, Hildner K, Ise W, Lee WL, et al. The AP-1 transcription factor Batf controls T(H)17 differentiation. *Nature*. 2009;460(7253):405–409.
45. Amir M, Chaudhari S, Wang R, et al. REV-ERBalpha regulates TH17 cell development and autoimmunity. *Cell Rep*. 2018;25(13):3733–3749.e8.
46. Ciofani M, Madar A, Galan C, et al. A validated regulatory network for Th17 cell specification. *Cell*. 2012;151(2):289–303.
47. Shi L, Wang JM, Ren JP, et al. KLRG1 impairs CD4+ T cell responses via p16ink4a and p27kip1 pathways: Role in hepatitis B vaccine failure in individuals with hepatitis C virus infection. *J Immunol*. 2014;192(2):649–657.
48. Horton JS, Yamamoto SY, Bryant-Greenwood GD. Relaxin modulates proinflammatory cytokine secretion from human decidual macrophages. *Biol Reprod*. 2011;85(4):788–797.
49. Belikan P, Buhler U, Wolf C, et al. CCR7 on CD4(+) T cells plays a crucial role in the induction of experimental autoimmune encephalomyelitis. *J Immunol*. 2018;200(8):2554–2562.
50. Carter SL, Muller M, Manders PM, Campbell IL. Induction of the genes for Cxcl9 and Cxcl10 is dependent on IFN-gamma but shows differential cellular expression in experimental autoimmune encephalomyelitis and by astrocytes and microglia in vitro. *Glia*. 2007;55(16):1728–1739.
51. Frank-Kamenetsky M, Zhang XM, Bottega S, et al. Small-molecule modulators of Hedgehog signaling: Identification and characterization of Smoothed agonists and antagonists. *J Biol*. 2002;1(2):10.
52. Das I, Park JM, Shin JH, et al. Hedgehog agonist therapy corrects structural and cognitive deficits in a Down syndrome mouse model. *Sci Transl Med*. 2013;5(201):201ra120.
53. Heine VM, Griveau A, Chapin C, Ballard PL, Chen JK, Rowitch DH. A small-molecule smoothed agonist prevents glucocorticoid-induced neonatal cerebellar injury. *Sci Transl Med*. 2011;3(105):105ra104.
54. Gaublotte JT, Yosef N, Lee Y, et al. Single-cell genomics unveils critical regulators of Th17 cell pathogenicity. *Cell*. 2015;163(6):1400–1412.
55. Hirota K, Duarte JH, Veldhoen M, et al. Fate mapping of IL-17-producing T cells in inflammatory responses. *Nat Immunol*. 2011;12(3):255–263.
56. Becher B, Tugues S, Greter M. GM-CSF: from growth factor to central mediator of tissue inflammation. *Immunity*. 2016;45(5):963–973.
57. Galli E, Hartmann FJ, Schreiner B, et al. GM-CSF and CXCR4 define a T helper cell signature in multiple sclerosis. *Nat Med*. 2019;25(8):1290–1300.
58. Wagner CA, Roque PJ, Goverman JM. Pathogenic T cell cytokines in multiple sclerosis. *J Exper Med*. 2020;217(1):e20190460.
59. Wang Y, Imitola J, Rasmussen S, O'Connor KC, Khoury SJ. Paradoxical dysregulation of the neural stem cell pathway sonic hedgehog-Gli1 in autoimmune encephalomyelitis and multiple sclerosis. *Ann Neurol*. 2008;64(4):417–427.
60. Yanez DC, Lau CI, Chawda MM, Ross S, Furmanski AL, Crompton T. Hedgehog signaling promotes TH2 differentiation in naive human CD4 T cells. *J Allergy Clin Immunol*. 2019;144(5):1419–1423.e1.
61. Restorick SM, Durant L, Kalra S, et al. CCR6(+) Th cells in the cerebrospinal fluid of persons with multiple sclerosis are dominated by pathogenic non-classic Th1 cells and GM-CSF-only-secreting Th cells. *Brain Behav Immunity*. 2017;64:71–79.
62. Duncker PC, Stoolman JS, Huber AK, Segal BM. GM-CSF promotes chronic disability in experimental autoimmune encephalomyelitis by altering the composition of central nervous system-infiltrating cells, but is dispensable for disease induction. *J Immunol*. 2018;200(3):966–973.
63. Ifergan I, Davidson TS, Kebir H, et al. Targeting the GM-CSF receptor for the treatment of CNS autoimmunity. *J Autoimmun*. 2017;84:1–11.
64. Knier B, Hiltensperger M, Sie C, et al. Myeloid-derived suppressor cells control B cell accumulation in the central nervous system during autoimmunity. *Nat Immunol*. 2018;19(12):1341–1351.
65. Li R, Rezk A, Miyazaki Y, et al. Proinflammatory GM-CSF-producing B cells in multiple sclerosis and B cell depletion therapy. *Sci Transl Med*. 2015;7(310):310ra166.
66. Ronchi F, Basso C, Preite S, et al. Experimental priming of encephalitogenic Th1/Th17 cells requires pertussis toxin-driven IL-1beta production by myeloid cells. *Nat Commun*. 2016;7:11541.
67. Levesque SA, Pare A, Mailhot B, et al. Myeloid cell transmigration across the CNS vasculature triggers IL-1beta-driven neuroinflammation during autoimmune encephalomyelitis in mice. *J Exper Med*. 2016;213(6):929–949.
68. Ponath G, Park C, Pitt D. The role of astrocytes in multiple sclerosis. *Front Immunol*. 2018;9:217.
69. Rothhammer V, Borucki DM, Tjon EC, et al. Microglial control of astrocytes in response to microbial metabolites. *Nature*. 2018;557(7707):724–728.
70. Pierson ER, Goverman JM. GM-CSF is not essential for experimental autoimmune encephalomyelitis but promotes brain-targeted disease. *JCI Insight*. 2017;2(7):e92362.
71. Lee W, Kim HS, Hwang SS, Lee GR. The transcription factor Batf3 inhibits the differentiation of regulatory T cells in the periphery. *Exper Mol Med*. 2017;49(11):e393.
72. Komuczki J, Tuzlak S, Friebel E, et al. Fate-mapping of GM-CSF expression identifies a discrete subset of inflammation-driving T helper cells regulated by cytokines IL-23 and IL-1beta. *Immunity*. 2019;50(5):1289–1304.e6.
73. Hartmann FJ, Khademi M, Aram J, et al. Multiple sclerosis-associated IL2RA polymorphism controls GM-CSF production in human TH cells. *Nat Commun*. 2014;5:5056.
74. Sheng W, Yang F, Zhou Y, et al. STAT5 programs a distinct subset of GM-CSF-producing T helper cells that is essential for autoimmune neuroinflammation. *Cell Res*. 2014;24(12):1387–1402.
75. International Multiple Sclerosis Genetics C, Hafler DA, Compston A, et al. Risk alleles for multiple sclerosis identified by a genomewide study. *N Engl J Med*. 2007;357(9):851–862.
76. Katzman SD, Hoyer KK, Dooms H, et al. Opposing functions of IL-2 and IL-7 in the regulation of immune responses. *Cytokine*. 2011;56(1):116–121.

77. Campbell IK, van Nieuwenhuijze A, Segura E, et al. Differentiation of inflammatory dendritic cells is mediated by NF-kappaB1-dependent GM-CSF production in CD4 T cells. *J Immunol.* 2011;186(9):5468–5477.
78. Yu J, Zhou X, Nakaya M, Jin W, Cheng X, Sun SC. T cell-intrinsic function of the noncanonical NF-kappaB pathway in the regulation of GM-CSF expression and experimental autoimmune encephalomyelitis pathogenesis. *J Immunol.* 2014;193(1):422–430.
79. Hayden MS, Ghosh S. NF-kappaB, the first quarter-century: Remarkable progress and outstanding questions. *Genes Dev.* 2012;26(3):203–234.
80. Lee PW, Severin ME, Lovett-Racke AE. TGF-beta regulation of encephalitogenic and regulatory T cells in multiple sclerosis. *Eur J Immunol.* 2017;47(3):446–453.
81. Brechbiel J, Miller-Moslin K, Adjei AA. Crosstalk between hedgehog and other signalling pathways as a basis for combination therapies in cancer. *Cancer Treatment Rev.* 2014;40(6):750–759.
82. Singh VB, Singh MV, Gorantla S, Poluektova LY, Maggirwar SB. Smoothened agonist reduces human immunodeficiency virus type-1-induced blood-brain barrier breakdown in humanized mice. *Sci Rep.* 2016;6:26876.